

# Reversible Data Hiding with Different Embedding Capacity based on Optimal Embedding Strategy Selection and Image Quality Assessment Criteria

Yang Yang

School of electronics and information engineering  
Anhui University  
111 Jiulong Road, Jingkai District, Hefei, China  
sky\_yang@ahu.edu.cn

Xue Cai, Mingxu Zhang and Xingxing Xiao

cedartsia@163.com; mingxu\_zhang@yeah.net; xiaoxingxiaabb@163.com

Received July 2018; revised December 2018

---

**ABSTRACT.** *Reversible data hiding (RDH) has been a spotlight in the past decade. Most of RDH algorithms aim at achieving higher embedding capacity (EC) with lower distortion. However, little of the algorithms takes into account adaptively embedding at low and high EC simultaneously, which leads these algorithms to achieve better performance only at low EC or high EC. In this paper, we proposed an RDH algorithm with different EC based on optimal embedding strategy selection and image quality assessment criteria. The proposed method adaptively selects the optimal embedding strategy between prediction-error-shifting-based (PES-based) adaptive embedding method and prediction-error-expansion-based (PEE-based) adaptive embedding method according to EC and different image quality assessment (IQA) criteria. In addition to the traditional peak signal-to-noise ratio (PSNR) criterion, two no-reference IQA methods for selecting the optimal embedding strategy and assessing the quality of marked images are applied in this paper, which are more consistent with human visual system (HVS), blind image spatial quality evaluator (BRISQUE) and natural image quality evaluator (NIQE). The experiments at low EC and high EC show that the proposed method can achieve better image quality when compared with other related RDH methods.*

**Keywords:** Reversible data hiding, Optional embedding strategy, Different embedding capacity, Image quality assessment criterion, Prediction error

---

**1. Introduction.** RDH is one kind of information hiding techniques with the characteristics such that not only the secret data need to be precisely extracted, but also the cover image itself should be restored lossless. In some fields, such as legal evidence, military imagery and law forensics, it is not allowed to make even a little modification in the image. Hence, RDH is particularly important.

EC and image distortion are important metrics to evaluate the performance of RDH. In fact, increasing EC often causes more distortion in image content. In most literatures on RDH, the quality of the marked image is assessed by PSNR. PSNR is a traditional IQA method belong to the full-reference IQA. However, it is based on the error between the corresponding pixels, and does not take the characteristics of the HVS into consideration, so the evaluation results are not consistent with the subjective feeling of human eye sometimes. It has been demonstrated that BRISQUE in [1] and NIQE in [2] perform quite

well in terms of correlation with human perception. Hence, BRISQUE and NIQE are also adopted to assess image quality in this paper. BRISQUE based on natural scene statistic (NSS) operates in the spatial domain, and the empirical distribution of locally normalized luminances and products of locally normalized luminances under a spatial NSS model are used to compute quality features. NIQE is based on the construction of a quality aware collection of statistical features based on space domain NSS model. It is completely blind because it only makes use of measurable deviations from statistical regularities observed in natural images, without training on human-rated distorted images. Generally, higher PSNR, lower BRISQUE and NIQE denote better image quality.

Most of the state-of-the-art RDH methods aim at providing a good performance in higher EC and less image distortion [3-5]. Based on this purpose, many RDH methods on image have been proposed. The part of RDH methods are realized through a process of semantic lossless compression [6-8], in which some space is saved for embedding extra data by lossless compressing the image. The compressed image should be as close as possible to the original image, so one can get a marked-image with good quality. The other part of RDH methods are achieved in image spatial domain and they have two major approaches: histogram shifting (HS) and difference expansion (DE). A histogram is first generated for the methods based on HS, and then reversible data embedding is realized by modifying the histogram. HS-based RDH is first proposed by Ni et al. in [9]. So far, Ni et al.'s HS method is extensively investigated and many subsequent works are proposed. In [10], Fallahpour et al. proposed to divide image into blocks. For each block, the histogram is generated and Ni et al.'s method [9] is applied for each block for data embedding. In [11], Xuan et al. proposed a new HS-based method, which is based on modification of the histogram generated from high-frequency IWT coefficients. DE-based RDH is firstly proposed by Tian et al. in [12-13] and it performs better by providing a higher EC while keeping the distortion low when compared with the lossless compression. In [14], DE is improved by using two different integer-to-integer transformations of pixels considering the magnitude of difference, which is based on invariability of the sum of pixel pair and pairwise difference adjustment. Prediction-error-expansion (PEE) is firstly proposed by Thodi and Rodriguez in [15] and [16], and this technique has been widely adopted by many subsequent RDH works [17-39]. In order to generate a sharply distributed prediction-error histogram, [30-33] focus on exploiting the advanced prediction techniques. In [33], Qin et al.'s method proposed an inpainting-assisted prediction rule, and the image inpainting technique is based on partial differential equations.

On the one hand, some algorithms only apply to low ECs [34-36]. Among these methods, [34] proposed an efficient reversible data hiding based on multiple histograms modification. In his method, complexity measurement is calculated for each pixel, and pixels are divided into several set according to the complexity. PEE is applied for each pixels set. Li et al.'s method [35] and Jung et al.'s method [36] have proposed RDH methods based on pixels-value-ordering, which can modify at most half of the pixels in an image. In [35], cover image is divided into no-overlapping blocks. In each block, pixels are sorted in ascending order. Then, maximum and minimum of pixels are predicted by the second largest pixel and second smallest pixel respectively. According to the max and min PEs, PEE is used to hide a secret bit. Only the max PE values 1 and min PE values -1 are used to embed. Finally, 2 bits can be embedded into each block. The difference between [35] and [36] is that each block contains four pixels in [35] while three pixels in [36]. It is clear that the highest EC depends on the number of max and min PEs. That is to say, a higher EC can not be achieved (for example, the maximum embedding capacity is 0.21 bpp for Lena in [36]). As a result, Li et al.'s method [35] and Jung et al.'s method [36] can not achieve higher EC.

On the other hand, some of these algorithms [25,29,32,37,39] applied to high EC are proposed. Peng et al.'s method in [25] is based on adaptive embedding and integer transform, which embeds message into a  $n$ -sized image block. Li et al.'s method [29] proposed an efficient RDH method by incorporation adaptive embedding and pixels selection in PEE. In [32], Luo et al.'s method proposed an interpolation-based prediction rule. In his method, the prediction error is calculated as the weighted average of its nearest pixels. Sachnev et al.'s method [37] have proposed an RDH using pixel sorting and PEE. Using sorting is beneficial to embed data into the pixels which located in smooth region. Besides, the thresholds pair is  $(-1, 0)$  at low EC, which means the pixels with PE smaller than  $-1$  or higher than  $0$  are shifted for embedding. Most of these shifted pixels are unnecessary to be modified, which leads to lower PSNR. With the increasing of EC, the pixels located in texture region are selected to embed all of the secret data, which leads to more modification and visual distortion of marked image. Hence, the embedding performance is not satisfactory in high EC due to its own characteristics. In a word, Sachnev et al.'s method [37] causes unnecessary image modification at low EC and rapid distortion with EC increased. Wu et al. in [39] proposed a RDH based on prediction errors by efficient histogram modification. Embedding with prediction errors is investigated with four prediction modes. In His method, some prediction errors are calculated by the two neighboring pixels and the other pixels are computed by the four pixels along the  $45^\circ$  and  $135^\circ$  diagonal direction pixels. Hence, the prediction performance is weaker than Sachnev et al.'s method, which results in more modification at low EC.

In order to achieve better embedding performance both at high EC and low EC, Weng et al.'s method [38] has proposed an optional embedding strategy to select a low-distortion RDH method according to the desired EC. DE is selected to embed data in the smooth region at low EC. When EC approaches gradually to the maximum EC of DE, adaptive embedding proposed by Li at al.'s method [29] is employed to embed data instead of DE. The performance of the optional embedding strategy at low EC is not as well as that at high EC, this is because the thresholds of DE are selected from the center of prediction error histogram (PEH), which leads to shift pixels located in both sides of PEH. As we all know, modifying more pixels results in worse image quality. Hence, the performance at low EC of optional embedding strategy is not always better than Sachnev et al.'s method.

As mentioned before, little of the algorithm takes into account adaptively embedding for low and high EC. Hence, optional embedding strategy based on IQA criterion with different EC is proposed in this paper. One of PES-based adaptive embedding and PEE-based adaptive embedding is selected according to EC. For PES-based adaptive embedding, the thresholds  $(t_1, t_2, t_1 < t_2)$  are selected outside the PEH to decrease image distortion. Only the pixels with  $PEs \in (-\infty, t_1) \cup (t_2, +\infty)$  are shifted outward of the PEH. In this way, the number of modified pixels is decreased. For PEE-based embedding, pixels are divided into the smooth region and the texture region. As we all know, PEH of the smooth region is much sharper than that of the texture region. In order to increase EC, 2 bits are embedded into the smooth region and 1 bit is embedded into the texture region. This is because the additional distortion due to embedding 2 bits message into the smooth region is smaller than that in the texture region (which is demonstrated at section 2.2.2). Besides, in order to satisfy different IQA criterion, the embedding procedure is selected according to the employed IQA criterion at low EC, which means the embedding procedure is opted by different IQA criterion. In general, PSNR is popularly used in most RDH algorithms. In this paper, another two no-reference IQA methods (BRISQUE and NIQE) which are based on NSS are employed to select embedding procedure at low EC. If PSNR is employed to assess image quality, then the optimal embedding procedure is

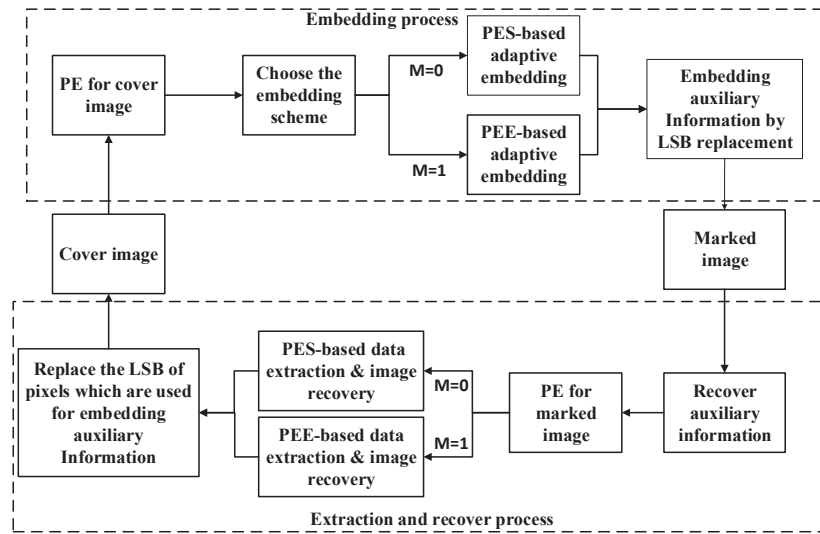


FIGURE 1. process of the proposed method

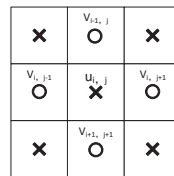


FIGURE 2. Interpolate technique to get PE

selected according to the results of PSNR. And so on, for each of the other two IQA methods. Experimental results show that our method is effective due to selecting embedding procedure according to EC and different IQA criterion.

This paper is organized as follows. In section 2, we elaborate proposed method. The performance of the proposed method is evaluated and compared with the other methods in Section 3, and the conclusion is finally presented in Section 4.

**2. Proposed method.** Fig.1 shows the process of the proposed method, where  $M$  denotes the embedding strategy which is adopted according to EC and IQA criteria. Before embedding, PE is calculated for cover image. A sharply distributed PEH is to the benefit of embedding performance with a better quality of marked image, so a more accurate prediction rule is put to use in this paper. As our purpose is to reduce the embedding distortion by decreasing modification of pixels, different embedding process is adopted according to EC. In order to extract the data and recover image, some auxiliary information needs to be embedded into the image by least significant bit (LSB) replacement.

**2.1. Calculating prediction rule.** As we all know, the more accurate the PE is, the better the embedding performance is. Luo et al.'s method [32] proposed the first RDH scheme using interpolation technique to obtain PE, which increases the accuracy of PE. Hence, in order to improve the prediction-accuracy, interpolation technique is adopted to obtain PE.

The cover image is divided into Cross X and Dot O. Note that the two sets (the Cross set and Dot set) are independent of each other. Independence means changes in one set do not affect the other set, and vice versa. In the first layer, Pixels from the Dot set are used for computing predicted values  $u'_{i,j}$ , whereas pixels from the Cross set  $u_{i,j}$  are used for embedding data. And pixels modified from Cross set are used for computing predicted values of Dot set in the second layer. Since the two layers' embedding processes are similar, we only take the Cross layer for illustration.

The prediction value  $u'_{i,j}$  in Fig.2 is computed using its four nearest Dot pixels ( $V_{i,j-1}, V_{i,j+1}, V_{i+1,j}, V_{i-1,j}$ ):

$$u'_{i,j} = x_0 \left( \frac{\sigma_2}{\sigma_1 + \sigma_2} \right) + x_{90} \left( \frac{\sigma_1}{\sigma_1 + \sigma_2} \right) \quad (1)$$

where

$$x_0 = \frac{V_{i,j+1} + V_{i,j-1}}{2} \quad (2)$$

$$x_{90} = \frac{V_{i+1,j} + V_{i-1,j}}{2} \quad (3)$$

$$\sigma_1 = \frac{(V_{i,j-1} - \mu)^2 + (x_0 - \mu)^2 + (V_{i,j+1} - \mu)^2}{3} \quad (4)$$

$$\sigma_2 = \frac{(V_{i-1,j} - \mu)^2 + (x_{90} - \mu)^2 + (V_{i+1,j} - \mu)^2}{3} \quad (5)$$

$$\mu = \frac{V_{i,j-1} + V_{i,j+1} + V_{i-1,j} + V_{i+1,j}}{4} \quad (6)$$

$x_0$  and  $x_{90}$  represent the interpolation values along  $0^\circ$  diagonal and  $90^\circ$  diagonal directions, respectively.  $V_{i,j-1}, V_{i,j+1}, V_{i+1,j}, V_{i-1,j}$  are left, right, top and bottom neighbor pixels of  $u_{i,j}$ .  $\mu$  is the mean value of  $V_{i,j-1}, V_{i,j+1}, V_{i+1,j}$  and  $V_{i-1,j}$ .  $\sigma_1$  and  $\sigma_2$  are the variance estimation of interpolation errors in two diagonal directions, respectively. The PE  $e_{i,j}$  is computed as:

$$e_{i,j} = u_{i,j} - u'_{i,j} \quad (7)$$

**2.2. Embedding procedure.** The distortion is reduced with the decrease of image modification. With EC increased, the causation of distortion is changed. But we can simply sum up into two situations: One is that distortion is mainly caused by shifting pixels for embedding with low EC. Another one is that most of the pixels are modified for data embedding at high EC, which means the distortion is mainly caused by embedding rather than shifting. So we need to decrease the amount of shifted pixels at low EC and expansion pixels at high EC. Hence, concerning the problem that the cause of distortion is not same at different EC, and reducing the maximum modification pixels, two embedding processes are proposed for selection.

**2.2.1. PES-based adaptive embedding method.** At low EC, in order to decrease the number of shifted pixels, we prior to selecting bins at two sides of the PEH by HS to embed data. The cover image is divided into Cross and Dot set and embedding thresholds are selected according to EC. Just as section 2.1, we only take the Cross layer for illustration. The embedding rule is as follows.

Suppose that  $t_1$  and  $t_2$  are the embedding parameters selected for embedding data. All bins  $e_{i,j} \in (-\infty, t_1) \cup (t_2, +\infty)$  are shifted outward, and bins  $e_{i,j} \in (t_1, t_2)$  are unchanged

while bins  $e_{i,j} = t_1$  and  $e_{i,j} = t_2$  are used to embed data as follows:

$$e'_{i,j} = \begin{cases} e_{i,j} - 1 & \text{if } e_{i,j} < t_1 \\ e_{i,j} - b & \text{if } e_{i,j} = t_1 \\ e_{i,j} & \text{if } t_1 < e_{i,j} < t_2 \\ e_{i,j} + b & \text{if } e_{i,j} = t_2 \\ e_{i,j} + 1 & \text{if } e_{i,j} > t_2 \end{cases} \quad (8)$$

where  $b \in \{0, 1\}$  is the message bit.

The marked image  $U_{i,j}$  is calculated as  $U_{i,j} = u'_{i,j} + e'_{i,j}$ .

The choice of  $t_1$  and  $t_2$  is a key issue because it directly affects the number of shifted pixels. As mentioned before, distortion can be reduced by decreasing image modification no matter which IQA criterion is employed. Hence,  $t_1$  and  $t_2$  with minimum image modification should be selected. Generally, the thresholds of most of the state-of-art RDH algorithms are selected from the center of PEH, such as Li et al.'s method [35], Jung et al.'s method [36] and Sachnev et al.'s method [37]. All bins  $e_{i,j} \in (-\infty, t_1) \cup (t_2, +\infty)$  are shifted outward for Sachnev et al.'s method. And bins  $e_{i,j} \in (t_1, t_2)$  are expanded to embed data for Sachnev et al.'s method [37].  $t_1$  and  $t_2$  default to -1 and 0 respectively for Sachnev et al.'s method [37]. With EC increased,  $t_1$  and  $t_2$  are selected from the center to two sides of PEH. For Jung et al.'s method [36] and Li et al.'s method [35], All bins  $e_{i,j} \in (-\infty, t_1) \cup (t_2, +\infty)$  are shifted outward, and only pixels with  $e_{i,j} = t_1$  and  $e_{i,j} = t_2$  can be used to embed data for while others are not changed.  $t_1$  and  $t_2$  are always -1 and 1 respectively. As we can see, all of three methods' thresholds are selected in the center of PEH, which means most of bins on both sides of thresholds need to be shifted outward.

Hence, in order to decrease the number of modified pixels, thresholds are selected from the outward of PEH for the proposed PES-based adaptive embedding. The initial values of thresholds are the min value and max value of PE respectively. Then find the final thresholds which can satisfy EC with the minimum amount of shifted pixels, which means the minimum number of  $e_{i,j} \in (-\infty, t_1) \cup (t_2, +\infty)$ , such that

$$\begin{aligned} & \text{minimize } \sum_{e_{i,j} < t_1} h(e_{i,j}) + \sum_{e_{i,j} > t_2} h(e_{i,j}) \\ & \text{subject to } h(t_1) + h(t_2) \geq EC \end{aligned} \quad (9)$$

where  $EC$  donates the embedding capacity, and  $h(e_{i,j})$  donates the number of pixels with PE valued  $e_{i,j}$ .  $h(t_1)$  and  $h(t_2)$  donate the number of pixels with PE valued  $t_1$  and  $t_2$  respectively.

We take an example to illustrate the advantage of PES-based adaptive embedding intuitively. Suppose that Fig.3 is the PEH of cover image. Table 1 shows the number of shifted pixels with different EC for Li et al.'s method [35], Jung et al.'s method [36], Sachnev et al.'s method [37], and the proposed method. As we can see, the number of shifted pixels is not changed with EC increased for Li et al.'s [35], Jung et al.'s [36] and Sachnev et al.'s [37]. With EC increased from 9 bits to 58 bits,  $t_1$  and  $t_2$  of Sachnev et al.'s method are -1 and 0, which are -1 and 1 for Jung et al.'s method [36] and Li et al.'s method [35]. Meanwhile, the number of shifted pixels of Sachnev et al.'s method is always 207, which is 177 for Jung et al.'s method and Li et al.'s method. However, with EC increased, the number of shifted pixels is also increased for PES-based adaptive embedding. Besides,  $t_1$  and  $t_2$  are selected from the outside to center of PEH for PES-based adaptive embedding. When  $EC = 9$  bits,  $t_1 = -6$  and  $t_2 = 6$  can embed all data for PES-based embedding. Therefore, there is no need to shift pixels in PES-based adaptive embedding. When  $EC = 58$  bits,  $t_1$  and  $t_2$  are -1 and 1 respectively for PES-based adaptive embedding, which is as same as Jung et al.'s method [36]. This is because that

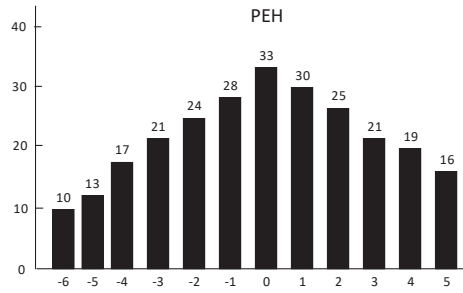


FIGURE 3. An example of shifted pixels

for Sachnev et al.'s method [35],  $t_1$  and  $t_2$  default to -1 and 0, so the number of shifted pixels is all the pixels with  $e_{i,j} < -1$  and  $e_{i,j} > 0$ . The pair of  $t_1$  and  $t_2$  is always -1 and 1 for Jung et al.'s method [36], which means the number of shifted pixels is all the pixels with  $e_{i,j} < -1$  and  $e_{i,j} > 1$ . For PES-based adaptive embedding,  $t_1$  and  $t_2$  are selected from the outward of PEH according to EC, so the number of shifted pixels is increased with EC, but the number of shifted pixels of the other three methods are not changed. In other words, the embedding cost of pixels is larger than PES-based adaptive embedding for all EC of Sachnev et al.'s method [37], Jung et al.'s method [36] and Li et al.'s method [35] at low EC, which leads to more image distortion.

TABLE 1. the number of shifted pixels with different EC for Li et al.'s[35], Jung et al.'s[36] Sachnev et al.'s[37] and the proposed method.

Method	EC(bits)	Thresholds	Number of shifted pixels
Li's in [35]	9	(-1,1)	177
Li's in [35]	22	(-1,1)	177
Li's in [35]	35	(-1,1)	177
Li's in [35]	58	(-1,1)	177
Jung's in [36]	9	(-1,1)	177
Jung's in [36]	22	(-1,1)	177
Jung's in [36]	35	(-1,1)	177
Jung's in [36]	58	(-1,1)	177
Sachnev's in [37]	9	(-1,0)	207
Sachnev's in [37]	22	(-1,0)	207
Sachnev's in [37]	35	(-1,0)	207
Sachnev's in [37]	58	(-1,0)	207
the proposed method	9	(-6,6)	0
the proposed method	22	(-5,6)	10
the proposed method	35	(-4,4)	50
the proposed method	58	(-1,1)	177

Besides, as image quality is rapidly decreased when shifted more than one time, we only shift one time to embed data. That's why it is only applicable at low EC. With the increasing of EC, another embedding process is adopted in our methods, which is introduced in section 2.2.2.

*2.2.2. PEE-based adaptive embedding method.* As 2.2.1 introduced, PES-based adaptive embedding is only used at low EC. However, with EC increased, a larger proportion of PEs in the histogram are modified to embed data. In order to decrease the amount of

	$X_{i-1,j}$		$X_{i-1,j+2}$
$X_{i,j-1}$	$X_{i,j}$	$X_{i,j+1}$	$X_{i,j+2}$
$X_{i+1,j-1}$	$X_{i+1,j}$	$X_{i+1,j+1}$	$X_{i+1,j+2}$
$X_{i+2,j-1}$	$X_{i+2,j}$	$X_{i+2,j+1}$	$X_{i+2,j+2}$

FIGURE 4. Calculation of smoothness

modified pixels, PEE-based adaptive embedding is adopted at high EC. As we all know, pixels located in the smooth region are similar, so the predicted values are close to original pixel. As a result, PEs tend to be 0. In other words, the distribution of PEH in the smooth region is concentrated in the center, i.e. the distribution of PEH has a sharp Laplacian distribution, which results in diminishing the amount of shifted pixels and leading to better image quality.

With EC increased, some pixels need to be embedded 2 bits to satisfy desired EC. In order to obtain a marked image with less distortion, we need to select the embedded pixels with less distortion. Hence, the additional distortion due to embed 2 bits message is calculated as follows:

$$AD(e_{i,j}) = \frac{1}{4} \sum_{b_1, b_2 \in \{0,1\}} (3e_{i,j} + 2b_1 + b_2)^2 - \frac{1}{2} \sum_{b \in \{0,1\}} (e_{i,j} + b)^2 = 8e_{i,j}^2 + 8e_{i,j} + 3 \quad (10)$$

As we can see, the smaller absolute value of  $e_{i,j}$  can get a smaller  $AD$ , which means less distortion. As mentioned before, PEs in the smooth region are smaller than these in the texture region, which means that the additional distortion due to embedding 2 bits message into the smooth region is smaller than that in the texture region. Hence, 2 bits are embedded into the pixels located in the smooth region and 1 bit is embedded into pixels located in the texture region.

The classification of smoothness and texture is another key issue for embedding performance. In this section, classification of smoothness and embedding process is introduced.

#### a Smoothness classification

It is well known that accuracy is improved with more pixels participating in the operation. More accurate smoothness measurement helps divide pixels which are similar to those around the pixel into the smooth region. The predicted value of pixels located in the smooth region is close to cover pixel. Further, a sharper Laplacian distribution PEH in the smooth region is obtained, which results in better image quality. Hence, in order to improve the accuracy of classification of smoothness, a more accurate smoothness measurement in [34] is adopted which is calculated as follows.

For the smoothness measurement  $n_{i,j}$ , it is computed based on a pixel context as shown in Fig.4. Specifically, it is defined as the sum of both vertical and horizontal absolute differences of every two consecutive pixels in the context of  $X_{i,j}$  consisting of 12 pixels as shown in Fig.4 according to eq(13).

$$\begin{aligned} V_{i,j} = & |X_{i,j-1} - X_{i+1,j-1}| + |X_{i+1,j-1} - X_{i+2,j-1}| + |X_{i+1,j} - X_{i,j+1}| \\ & + |X_{i,j+1} - X_{i+1,j+1}| + |X_{i+1,j+1} - X_{i+2,j+1}| + |X_{i-1,j+2} - X_{i,j+2}| \\ & + |X_{i,j+2} - X_{i+1,j+2}| + |X_{i+1,j+2} - X_{i+2,j+2}| \end{aligned} \quad (11)$$

$$\begin{aligned}
H_{i,j} &= |X_{i,j+1} - X_{i,j+2}| + |X_{i+1,j-1} - X_{i+1,j}| + |X_{i+1,j} - X_{i+1,j+1}| \\
&+ |X_{i+1,j+1} - X_{i+1,j+2}| + |X_{i+2,j-1} - X_{i+2,j}| + |X_{i+2,j} - X_{i+2,j+1}| \\
&+ |X_{i+2,j+1} - X_{i+2,j+2}|
\end{aligned} \tag{12}$$

$$n_{i,j} = V_{i,j} + H_{i,j} \tag{13}$$

In order to classify the pixel into the smooth region and the texture region,  $n_{i,j}$  will be scaled to 2 values. Firstly, select the threshold  $S$  as

$$S = \arg \min_n \left\{ \frac{\#\{1 \leq i \leq W, 1 \leq j \leq H : n_{i,j} \leq n\}}{W \times H} \geq \frac{1}{2} \right\} \tag{14}$$

where  $W$  and  $H$  are the size of cover image,  $\#$  means the cardinal number of a set.  $S$  is the min smoothness with the least amount of pixels when eq(14) holds.

Then we get 2 intervals  $[0, S], [S + 1, +\infty]$ , if a pixel with smoothness  $n_{i,j} \in [0, S]$ , it is located in the smooth region, otherwise, it is in the texture region.

### b Embedding procedure

After classifying pixels into the smooth region and texture region, two PEHs (PEH of the smooth region and the texture region) can be obtained. Generally, a more concentrated PEH helps reduce the number of shifted pixels. So the distortion of embedding 1 bit into the smooth region is much smaller than that into texture region. Besides, when EC is larger than 1bpp, embedding 1 bit into each expanded pixel for one round is not enough, but embedding 2 rounds i.e. embedding 2 bits into pixels, results in huge distortion. As mentioned before, the additional distortion due to embedding 2 bits message into the smooth region is smaller than that into texture region. Hence, 2 bits are embedded into the pixels located in smooth region due to that the PEH of smooth region has a sharper Laplacian distribution which leads to less shifted pixels.

For any pixel located in smooth region with  $e_{i,j} \in [-T_{adaptive}, T_{adaptive})$  ( $T_{adaptive}$  is the selected threshold to decide whether the bin is used to embed data.), 2 bits are embedded into  $e_{i,j}$ , so  $e_{i,j}$  is double expanded according to eq(15). If  $e_{i,j} \in (-\infty, -T_{adaptive} - 1]$  or  $e_{i,j} \in [T_{adaptive}, +\infty)$ , it will be shifted by  $3T_{adaptive}$ . Correspondingly, the modified PE is calculated as follows:

$$e'_{i,j} = \begin{cases} 4 \times e_{i,j} + b & \text{if } e_{i,j} \in [-T_{adaptive}, T_{adaptive}) \\ e_{i,j} - 3 \times T_{adaptive} & \text{if } e_{i,j} \leq -T_{adaptive} - 1 \\ e_{i,j} + 3 \times T_{adaptive} & \text{if } e_{i,j} \geq T_{adaptive} \end{cases} \tag{15}$$

where  $b \in \{0, 1, 2, 3\}$  is the message to be embedded.

For any pixel located in texture region with PE  $e_{i,j} \in [-T_{adaptive}, T_{adaptive})$ , 1 bit is embedded into  $e_{i,j}$ . If  $e_{i,j} \in (-\infty, -T_{adaptive} - 1]$  or  $e_{i,j} \in [T_{adaptive}, +\infty)$ , it will be shifted by  $T_{adaptive}$ . The modified PE is calculated as follows:

$$e'_{i,j} = \begin{cases} 2 \times e_{i,j} + b & \text{if } e_{i,j} \in [-T_{adaptive}, T_{adaptive}) \\ e_{i,j} - T_{adaptive} & \text{if } e_{i,j} \leq -T_{adaptive} - 1 \\ e_{i,j} + T_{adaptive} & \text{if } e_{i,j} \geq T_{adaptive} \end{cases} \tag{16}$$

where  $b \in \{0, 1\}$ .

Finally, calculate marked image  $U_{i,j}$  as PES-based adaptive embedding.

What we should take into consideration is the value of  $T_{adaptive}$ , which directly determines embedding performance. Since we are pursuing embedding more data with fewer modifications,  $T_{adaptive}$  for PEE-based embedding is selected from the center of PEH. If

$T_{adaptive}$  is selected from the side of PEH, embedding is purchased at too many modifications of expansion. In order to choose a threshold with least shifted pixels,  $T_{adaptive}$  is increased until  $T_{adaptive}$  can satisfy eq(17):

$$\begin{aligned} & \text{minimize } T_{adaptive} \\ & \text{subject to } 2h_s(e_s) + h_t(e_t) \geq EC \end{aligned} \quad (17)$$

where  $e_s \in [-T_{adaptive}, T_{adaptive})$  and  $e_t \in [-T_{adaptive}, T_{adaptive})$ ,  $h_s(e_s)$  and  $h_t(e_t)$  donate the number of pixels with  $-T_{adaptive} \leq e_{i,j} \leq T_{adaptive}$  in the smooth region and the texture region respectively.

2.2.3. *Selection of embedding process.* Decreasing the modification of pixels can effectively reduce image distortion. Adaptively selecting the best embedding process according to EC can efficiently reduce the impact of embedding data. In order to achieve better embedding performance, we need to consider that how to define high EC and low EC. Because shifting pixels more than once results in a rapid deterioration of image quality for PES-based adaptive embedding, the number of pixels with the value of highest two bins in PEH is defined as the boundary of high EC and low EC. In this section, the selection of embedding process is introduced respectively as follows.

1. At high EC, it means EC is larger than the number of pixels of the highest two bins in PEH. For PES-based adaptive embedding, shifting one time can not embed all data under this circumstance. Hence, PEE-based adaptive embedding is employed when eq(18) holds:

$$EC > h(e_{max1}) + h(e_{max2}) \quad (18)$$

where  $e_{max1}$  and  $e_{max2}$  donate the PE values of the highest two bins in PEH, and  $h(e_{max1})$  and  $h(e_{max2})$  donate the number of pixels with PE valued  $e_{max1}$  and  $e_{max2}$  respectively.

When eq(18) holds, it means shifting one time can not embed all data for PES-based embedding and we define it as high EC. As mentioned before, for PES-based adaptive embedding, the pixel shifted more than once will lead to rapid deterioration of image quality. Besides, PEE-based adaptive embedding classifies pixels into the smooth region and the texture region. 2 bits are embedded into the smooth region while 1 bit is embedded into texture region, which leads to a high EC with less modification of pixels. So if eq(18) holds, PEE-based adaptive embedding is adopted.

2. At low EC, it is not sure that which embedding process can achieve better result of IQA. Hence, embedding procedure is selected according to IQA criterion. The embedding procedure is selected according to eq(19) at low EC.

$$\begin{cases} EC \leq h(e_{max1}) + h(e_{max2}) \\ \text{optimal } \{Q_{PES}, Q_{PEE}\} \end{cases} \quad (19)$$

where  $Q$  donates the IQA criterion employed, *optimal* means the embedding procedure is selected with better image quality assessment results.

Notice that the higher PSNR, lower BRISQUE and NIQE donate better image quality. PSNR can reflect the error between the corresponding pixels, BRISQUE and NIQE perform quite well in terms of correlation with human perception. It means that the characteristics and emphasis of the three IQA criteria are different, so the embedding process is adaptively selected according to the employed IQA criterion. In other words, one of PES-based adaptive embedding and PEE-based adaptive embedding is selected according to different IQA criterion.

In summary, just as described in eq(19), embedding process is selected according to different IQA criterion of images at low EC.

As other RDH schemes, we also need a location map assigning 1s to record the positions of overflow/underflow pixels. And these pixels remain unchanged in the embedding process. The location map is compressed and its size is  $O_{flow}$ . In addition, in order to extract messages and recover cover image conveniently, we take  $M$  to donate the embedding process we employed.  $M = 1$  represents PEE-based embedding, or  $M = 0$  represents PES-based embedding. Besides, the auxiliary information is various for different embedding processes which is described as follows:

PEE-based adaptive embedding:

$M = 1$ ,  $T_{adaptive}$ ,  $S$ , size of compressed location map  $O_{flow}$  and compressed location map.

PES-based adaptive embedding:

$M = 0$ ,  $t_1$  and  $t_2$ , size of compressed location map  $O_{flow}$  and compressed location map.

The sizes of these auxiliary information are  $39 + O_{flow}$  bits and  $37 + O_{flow}$  bits respectively. And these information is recorded to replace the LSB of the first  $39 + O_{flow}$  or  $37 + O_{flow}$  pixels in cover image, the least signification bit (LSB) of the first  $39 + O_{flow}$  or  $37 + O_{flow}$  pixels  $S_{LSB}$  is also embedded as one part of the payload.

**2.3. Data extraction and cover restoration.** Due to using the interpolation technique to get PE, two sets (Cross and Dot set) are independent. Hence, the double decoding scheme is the inverse of the double encoding scheme. If Cross set is embedded firstly, Dot set is recovered firstly. Computations for Dot and Cross decoding schemes are similar. We just take Cross set as an example.

#### Step 1 extraction of the auxiliary information

Read LSB of the first pixel of marked image to  $M$ .

If  $M = 1$ , then read LSB of next  $38 + O_{flow}$  pixels of marked image to get  $T_{adaptive}$ ,  $S$ , size of compressed location map  $O_{flow}$ , compressed location map.

If  $M = 0$ , then read LSB of next  $36 + O_{flow}$  pixel of marked image to get  $t_1$  and  $t_2$ , size of compressed location map  $O_{flow}$ , compressed location map.

#### Step 2 extraction of the payload

For each marked image, if its location is associated with 1 in the location map, then it is ignored, because these pixels stay unchanged in embedding process. Otherwise, the prediction-error of marked image is obtained as embedding process. For each of two embedding methods (namely PEE-based adaptive embedding and PES-based adaptive embedding), its corresponding data extraction and pixel restoration are described as follows respectively.

#### PEE-based adaptive embedding:

First, calculate the smooth measurement in an inverse order to embedding process, i.e. from right to left and bottom to up. If  $n_{i,j} \leq S$ , then  $e_{i,j}$  is retrieved as follows.

$$e_{i,j} = \begin{cases} \lfloor e'_{i,j}/4 \rfloor & \text{if } e'_{i,j} \in [-4T_{adaptive}, 4T_{adaptive} - 1] \\ e'_{i,j} + 3 \times T_{adaptive} & \text{if } e'_{i,j} \leq -4T_{adaptive} - 1 \\ e'_{i,j} - 3 \times T_{adaptive} & \text{if } e'_{i,j} \geq 4T_{adaptive} \end{cases} \quad (20)$$

Correspondingly, the embedded data are extracted by the following formula:  $b = e'_{i,j} - 4 \times \lfloor e'_{i,j}/4 \rfloor$ . Otherwise,  $e_{i,j}$  is retrieved as follows:

$$e_{i,j} = \begin{cases} \lfloor e'_{i,j}/2 \rfloor & \text{if } e'_{i,j} \in [-2T_{adaptive}, 2T_{adaptive} - 1] \\ e'_{i,j} + T_{adaptive} & \text{if } e'_{i,j} \leq -2T_{adaptive} - 1 \\ e'_{i,j} - T_{adaptive} & \text{if } e'_{i,j} \geq 2T_{adaptive} \end{cases} \quad (21)$$

The embedded bit is extracted as  $b = e'_{i,j} - 2 \times \lfloor e'_{i,j}/2 \rfloor$ .

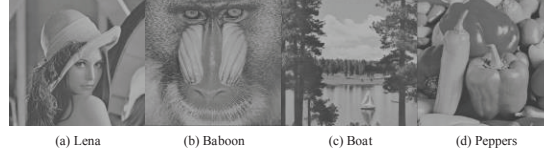


FIGURE 5. the original images

**PES-based adaptive embedding:** Calculate PE as  $e'_{i,j} = U_{i,j} - u'_{i,j}$  and embedded bit are retrieved as follows.

$$e_{i,j} = \begin{cases} e'_{i,j} + 1 & \text{if } e'_{i,j} < t_1 - 1 \\ t_1 & \text{if } e'_{i,j} = t_1 \text{ or } e'_{i,j} = t_1 - 1 \\ t_2 & \text{if } e'_{i,j} = t_2 \text{ or } e'_{i,j} = t_2 + 1 \\ e'_{i,j} - 1 & \text{if } e'_{i,j} > t_2 + 1 \end{cases} \quad (22)$$

$$b = \begin{cases} 1 & \text{if } e'_{i,j} = t_1 - 1 \\ 0 & \text{if } e'_{i,j} = t_1 \\ 0 & \text{if } e'_{i,j} = t_2 \\ 1 & \text{if } e'_{i,j} = t_2 + 1 \end{cases} \quad (23)$$

**Step3 restoration of the cover image** And recover original pixels by  $u_{i,j} = u'_{i,j} + e_{i,j}$ . When the current layer is fully extracted, classify the extracted bit stream into data bits and  $S_{LSB}$ , and restore the first  $39 + O_{flow}$  or  $37 + O_{flow}$  pixels by simple LSB replacement.

**3. Experimental result.** The images in experience are obtained from the network (<http://sipi.usc.edu/database>). In order to show the performance of proposed method, four images (Lena, Baboon, Boat and Peppers) with the size of  $512 \times 512$  are selected randomly. Besides, as our target is designing an algorithm with different embedding capacity based on optimal embedding strategy selection and IQA criteria, the proposed method is compared with Li et al.'s method [35], Jung et al.'s method [36], Sachnev et al.'s method [37] and Weng et al.'s method [38] at low EC, and with Sachnev et al.'s method [37] and Weng et al.'s method [38] at high EC. In Li et al.'s method [35] and Jung et al.'s method [36], the maximum EC are 26404 bits and 55358 bits respectively. Fig.6 shows the performance of the proposed method with different IQA criterion when compared with Li et al.'s method [35], Jung et al.'s method [36], Sachnev et al.'s method [37] and Weng et al.'s method [38] at low EC. Fig 7 shows the performance of the proposed method and Sachnev et al.'s method [37] and Weng et al.'s method [38] with the EC larger than the maximum EC of Jung et al.'s method [36] and Li et al.'s method [35], so Li et al.'s [35] method and Jung et al.'s method [36] are not contained. For convenience of description, Jung, Sachnev, Weng and Li are used as an abbreviation of Jung et al.'s, Sachnev et al.'s, Weng et al.'s and Li et al.'s.

Fig.6 shows PSNR, BRISQUE and NIQE three IQA criteria results between the proposed method and following four methods: Li's method [35], Jung's method [36], Sachnev's method [37] and Weng's method [38] at low EC. Due to the proposed method is adaptively select embedding process according to PSNR, BRISQUE and NIQE. We can clear see that the results of the proposed method are superior to Li's method [35], Jung's method [36], Sachnev's method [37] and Weng's method [38] for all test images and all IQA criteria, in which PSNR results are larger than the other RDH methods and BRISQUE and NIQE results are smaller than the other RDH methods. Lower values of BRISQUE and NIQE donate better image quality, while PSNR is higher. Hence, the proposed method achieves better performance no matter which IQA criterion is employed. This is

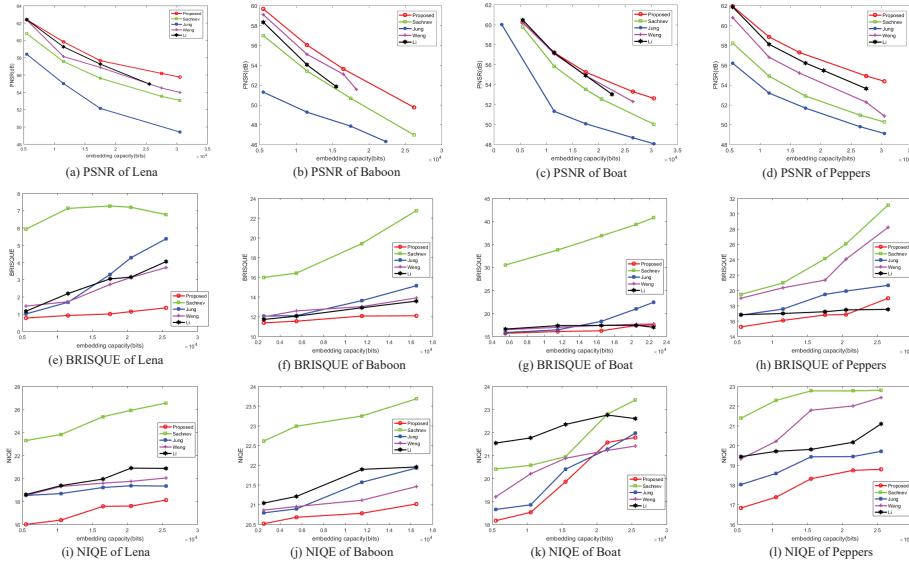


FIGURE 6. best PSNR, BRISQUE and NIQE between the proposed method and following four methods: Li et al.[35], Jung et al.[36], Sachnev et al.[37] and Weng et al.[38] at low EC

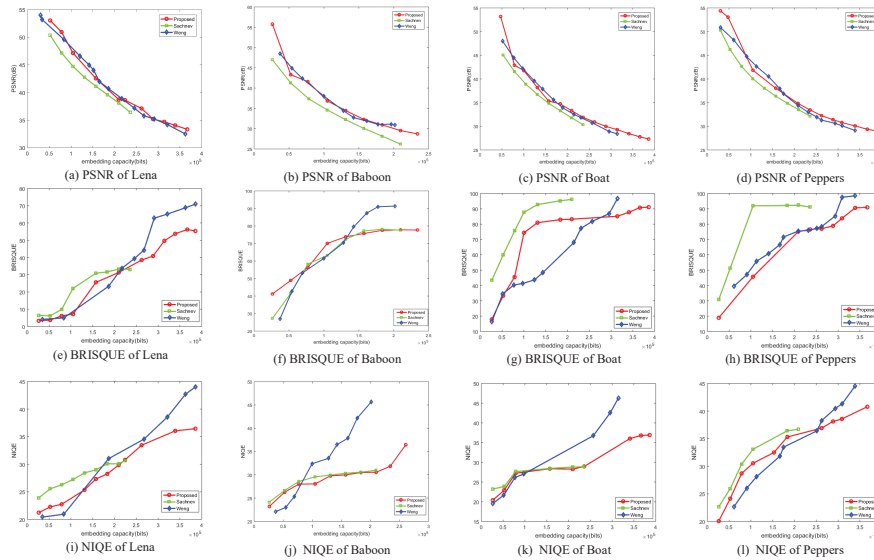


FIGURE 7. PSNR, BRISQUE and NIQE between the proposed method and following two methods: Sachnev et al.[37] and Weng et al.[38] at high EC

because that in Li’s method [35], cover image is divided into no overlapping blocks and pixels are sorted in ascending order in each block firstly. Then, maximum and minimum of pixels are predicted by the second largest pixel and second smallest pixel respectively. Finally, PEs valued 1 of max pixels and -1 of min pixels are used to embed secret data, PEs valued 0 remain unchanged while others are changed by 1. Hence, too many pixels are modified, which causes the image of the heave to be distorted. Jung’s method[36] is similar with Li’s method [35], it divides cover image into no overlapping sub-blocks that contain three pixels. Three pixels are sorted in ascending order to calculate PEs of max and min pixels. According to PEs, pixels-error expansion is used to hide a secret bit. The embedding process is as same as Li’s method [35]. Due to that the size of sub-blocks in Jung’s method [36] is smaller than that of Li’s method [35], the distortion is more

than Li's method [35]. In Sachnev's method [37], a sorting technique is combined into the rhombus pattern prediction technique, so that this method performs well and it is superior to Jung's method. For Sachnev's method [37], the pair of thresholds is  $(-1, 0)$ . As it is based on PEE, the PEs valued smaller than  $-1$  and larger than  $0$  are shifted. Besides, as the prediction rule in Sachnev's method is more accurate than Jung's method, the performance of Sachnev's method [37] is better than Jung's method [36]. Though Weng's method [38] uses an optional embedding strategy, DE is adopted to embed data at low EC, in which the threshold is selected from the center of PEH. Hence, the performance at low EC is similar with Sachnev's method [37]. In our method at low EC, we aim at selecting embedding process according to different IQA criterion. Different embedding processes with better value of PSNR, BRISQUE or NIQE are adaptively employed. The embedding process is opted on the basis of IQA criterion. As a result, our method realizes the best results of different IQA criterion compared with Li's method, Jung's method, Sachnev's method and Weng's method.

Fig.7 shows PSNR, BRISQUE and NIQE three IQA criteria results between the proposed method and following two methods: Sachnev's method [37] and Weng's method [39] at high EC, in which the EC that Li's method [35] and Jung's method [36] can't reach. As we can see, the results of proposed method significantly outperform Sachnev's method [37] method and achieves almost the same performance as Weng's method [38] at high EC. This is because that in Sachnev's method [37], it has to select those pixels in texture region for data embedding with EC increased, which leads to rapid deterioration of distortion. In Weng's method [38], it divided pixels into smoothness area and texture area, and used four prediction modes and adaptive embedding method in [29] to embed data at high EC, but local variance which used to estimate pixel's smoothness and texture is not accurate. In the proposed method, PEE-based adaptive embedding method is adopted at high EC, a more accurate smoothness and texture estimator is adopted. As a result, our method realizes the best results of different IQA criterion compared with Sachnev's method and closes to the results of Weng's method.

In a word, the proposed method focuses on increasing embedding performance with different EC. In order to get the best marked image at different EC, different embedding process is adopted according to IQA criterion, which are PES-based adaptive embedding and PEE-based adaptive embedding. For PES-based adaptive embedding, the thresholds are selected outside the PEH to decrease the number of shifted pixels which are not used for embedding. For PEE-based embedding, pixels are divided into the smooth region and texture region by a more accurate smoothness estimator, and 2 bits are embedded into the smooth region and 1 bit is embedded into the texture region. Due to that PES-based causes a rapid image distortion at high EC, PEE-based embedding is directly employed at high EC. Experimental result also demonstrates that the proposed method performs better than other RDH methods. That is because that the proposed method selects optimal embedding process adaptively according to embedding capacity with minimum distortion.

**4. Conclusions.** This paper proposes a novel RDH with different capacity based on optimal embedding strategy selection and image quality assessment criteria. At low EC, one of PEE-based adaptive embedding and PES-based adaptive embedding is selected according to different IQA criterion. For PES-based adaptive embedding, the thresholds are selected from the two sides to the center of PEH with the minimum shifted pixels. For PEE-based adaptive embedding, cover image is divided into the smooth region and the texture region. 2 bits are embedded into the smooth region and 1 bit is embedded into the texture region. Embedding procedure is selected according to different IQA criterion.

With EC increased, image quality is rapidly decreased when shifted more than one time for PES-based adaptive embedding. Hence, PEE-based adaptive embedding is employed automatically. The proposed method consists in selecting the optimal embedding process and has a better evaluation result between PEE-based adaptive embedding and PES-based adaptive embedding. In order to demonstrate the effectiveness of the proposed method, a series of experiments for low EC and high EC have been done in our experiment. The experiment demonstrates that the proposed method can achieve better image quality when compared with the state-of-art algorithms for low EC and high EC.

**Acknowledgment.** This work is partially supported by the Natural Science Foundation of China under Grant 61502007, partially by the Natural Science Research Project of Anhui province under Grant 1608085MF125, partially the NO.58 China Postdoctoral Science Foundation under Grant 2015M582015, partially by the backbone teacher training program of Anhui University, partially the Doctoral Scientific Research Foundation of Anhui University under Grant J01001319. The authors also gratefully acknowledge the helpful comments and suggestions of the reviewers, which have improved the presentation.

## REFERENCES

- [1] A. Mittal, A. K. Moorthy, A. C. Bovik, No-reference image quality assessment in the spatial domain, *IEEE Transactions on Image Processing A Publication of the IEEE Signal Processing Society*, vol. 21, no. 12, pp. 4695-4708, 2012.
- [2] A. Mittal, R. Soundararajan, A. C. Bovik, Making a completely blind image quality analyzer, *IEEE Signal Processing Letters*, vol. 20, no. 3, pp. 209-212, 2013.
- [3] C. Y. Yang, C. H. Lin, W. C. Hu, Reversible data hiding by adaptive iwt-coefficient adjustment, *Journal of Information Hiding and Multimedia Signal Processing*, vol. 2, no. 1, pp. 24-32, 2011.
- [4] H. C. Huang, F. C. Chang, Y. Y. Lu, Multi-bit reversible data hiding with prediction and difference alteration, *Journal of Information Hiding and Multimedia Signal Processing*, vol. 8, no. 2, pp. 435-444, 2017.
- [5] C. C. Luo, P. F. Shiu, High capacity data hiding scheme for dct-based images, *Journal of Information Hiding and Multimedia Signal Processing*, vol. 1, no. 3, 2010.
- [6] F. Willems, D. Maas, T. Kalker, Semantic lossless source coding, *Proc.allerton Conf.on Communication Control and Computing*, pp. Sept-oct, 2012.
- [7] W. Zhang, X. Hu, X. Li, N. Yu, Recursive histogram modification: establishing equivalency between reversible data hiding and lossless data compression, *IEEE Transactions on Image Processing*, vol. 22, no. 7, pp. 2775-2785, 2013.
- [8] C. Qin, Y. Hu, Reversible data hiding in VQ index table with lossless Coding and adaptive switching mechanism, *Signal Processing*, vol. 129, pp. 48-55, 2016.
- [9] Z. Ni, Y. Q. Shi, N. Ansari, W. Su, Reversible data hiding, *Proc. IEEE Int. Symp. Circuits Syst.*, vol. 2, pp. 912-915, 2003.
- [10] M. Fallahpour, M. H.Sedaaghi, High capacity lossless data hiding based on histogram modification, *Ieice Electron Express*, vol. 4, no. 7, pp. 205-210, 2007.
- [11] G. Xuan, Y. Q. Shi, P. Chai, X. Cui, Z. Ni, X. Tong, Optimum histogram pair based image lossless data embedding, *International Workshop on Digital Watermarking. Springer, Berlin*, pp. 264-278, 2007.
- [12] J. Tian, Wavelet-based reversible watermarking for authentication, *Security and Watermarking of Multimedia Contents IV*, pp. 679-690, 2002.
- [13] J. Tian, Reversible data embedding using a difference expansion, *IEEE Transactions on Circuits and Systems for Video Technology*, vol. 13, no. 8, pp. 890-896, 2003.
- [14] S. Weng, Y. Zhao, J. S. Pan, Reversible watermarking based on invariability and adjustment on pixel pairs, *IEEE Signal Processing Letters*, vol. 15, pp. 721-724, 2008.
- [15] D. M. Thodi, J. J. Rodriguez, Prediction-error based reversible watermarking, *International Conference on Image Processing. IEEE*, vol.3, pp. 1549-1552, 2005.
- [16] D. M. Thodi, J. J. Rodriguez, Expansion embedding techniques for reversible watermarking, *IEEE Trans Image Process*, vol. 16, no. 3, pp. 721-730, 2007.

- [17] Y. Yang, W. Zhang, D. Liang, N. Yu, A ROI-based high capacity reversible data hiding scheme with contrast enhancement for medical images, *Multimedia Tools and Applications*, vol. 77, pp. 10843-10865, 2018.
- [18] X. Gao, L. An, Y. Yuan, D. Tao, X. Li, Lossless data embedding using generalized statistical quantity histogram, *IEEE Transactions on Circuits and Systems for Video Technology*, vol. 21, no. 8, pp. 1061-1070, 2011.
- [19] J. Zhou, O. C. Au, Determining the capacity parameters in PEE-Based reversible image watermarking, *IEEE Signal Processing Letters*, vol. 19, no. 5, pp. 287-290, 2012.
- [20] I. C. Dragoi, D. Coltuc, Local-prediction-based difference expansion reversible watermarking, *IEEE Transactions on Image Processing A Publication of the IEEE Signal Processing Society*, vol. 23, no. 4, pp. 1779-1790, 2014.
- [21] I. C. Dragoi, D. Coltuc, On local prediction based reversible watermarking, *IEEE Trans. Image Process*, vol. 24, no. 4, pp. 1244-1246, 2015.
- [22] S. Xiang, Y. Wang, Non-integer expansion embedding techniques for reversible image watermarking, *Eurasip Journal on Advances in Signal Processing*, vol. 2015, no. 1, pp. 56, 2015.
- [23] S. Kim, X. Qu, V. Sachnev, H. J. Kim, Skewed histogram shifting for reversible data hiding using a pair of extreme predictions, *IEEE Transactions on Circuits and Systems for Video Technology*, doi: 10.1109/TCSVT.2018.2878932, 2018.
- [24] P. Puteaux, W. Puech, An efficient MSB prediction-based method for high-capacity reversible data hiding in encrypted images, *IEEE Transactions on Information Forensics and Security*, vol. 13, no. 7, pp. 1670-1681, 2018.
- [25] F. Peng, X. L. Li, B. Yang, Adaptive reversible data hiding scheme based on integer transform, *Signal Processing*, vol. 92, no. 1, pp. 54-62, 2012.
- [26] S. Weng, J. Pan, L. Li, Reversible data hiding based on an adaptive pixel-embedding strategy and two-layer embedding *Information Sciences*, vol. 369, pp. 144-159, 2016.
- [27] S. Weng, Y. Liu, J. S. Pan, Reversible data hiding based on flexible block-partition and adaptive block-modification strategy, *Journal of Visual Communication and Image Representation*, vol. 41, pp. 185-199, 2016.
- [28] S. Weng, J. S. Pan, Adaptive reversible data hiding based on a local smoothness estimator, *Multimedia Tools and Applications*, vol. 74, no. 23, pp. 10675-10678, 2015.
- [29] X. Li, B. Yang, T. Zeng, Efficient reversible watermarking based on adaptive prediction-error expansion and pixel selection, *IEEE Transactions on Image Processing A Publication of the IEEE Signal Processing Society*, vol. 20, no. 12, pp. 3524, 2011.
- [30] W. Wang, J. Ye, T. Wang, W. Wang, Reversible data hiding scheme based on significant-bit-difference expansion, *IET Image Processing*, vol. 11, no. 11, pp. 1002-1014, 2017.
- [31] H. Chen, J. Ni, W. Hong, T. Chen, High-Fidelity Reversible Data Hiding Using Directionally Enclosed Prediction, *IEEE Signal Processing Letters*, vol. 24, no. 5, pp. 574-578, 2017.
- [32] L. Luo, Z. Chen, M. Chen, X. Zeng, Z. Xiong, Reversible image watermarking using interpolation technique, *IEEE Transactions on Information Forensics and Security*, vol. 5, no. 1, pp. 187-193, 2010.
- [33] C. Qin, C. C. Chang, Y. H. Huang, L. T. Liao, An inpainting-assisted reversible steganographic scheme using a histogram shifting mechanism, *IEEE Transactions on Circuits and Systems for Video Technology*, vol. 23, no. 7, pp. 1109-1118, 2013.
- [34] X. Li, W. Zhang, X. Gui, B. Yang, Efficient reversible data hiding based on multiple histograms modification, *IEEE Transactions on Information Forensics and Security*, vol. 10, no. 9, pp. 2016-2027, 2017.
- [35] X. Li, J. Li, B. Li, B. Yang, High-fidelity reversible data hiding scheme based on pixel-value-ordering and prediction-error expansion, *Signal Processing*, vol. 93, no. 1, pp. 198-205, 2013.
- [36] K. H. Jung, A high-capacity reversible data hiding scheme based on sorting and prediction in digital images, *Multimedia Tools and Applications*, vol. 76, no. 11, pp. 1-11, 2017.
- [37] V. Sachnev, H. J. Kim, J. Nam, S. Suresh, Y. Q. Shi, Reversible watermarking algorithm using sorting and prediction, *IEEE Transactions on Circuits and Systems for Video Technology*, vol. 19, no. 7, pp. 989-999, 2009.
- [38] S. Weng, J. S. Pan, L. Zhou, Reversible data hiding based on the local smoothness estimator and optional embedding strategy in four prediction modes, *Multimedia Tools and Applications*, vol. 76, no. 11, pp. 1-23, 2016.
- [39] H. Wu, J. Huang, Reversible image watermarking on prediction errors by efficient histogram modification, *Signal Processing*, vol. 92, no. 12, pp. 3000-3009, 2012.